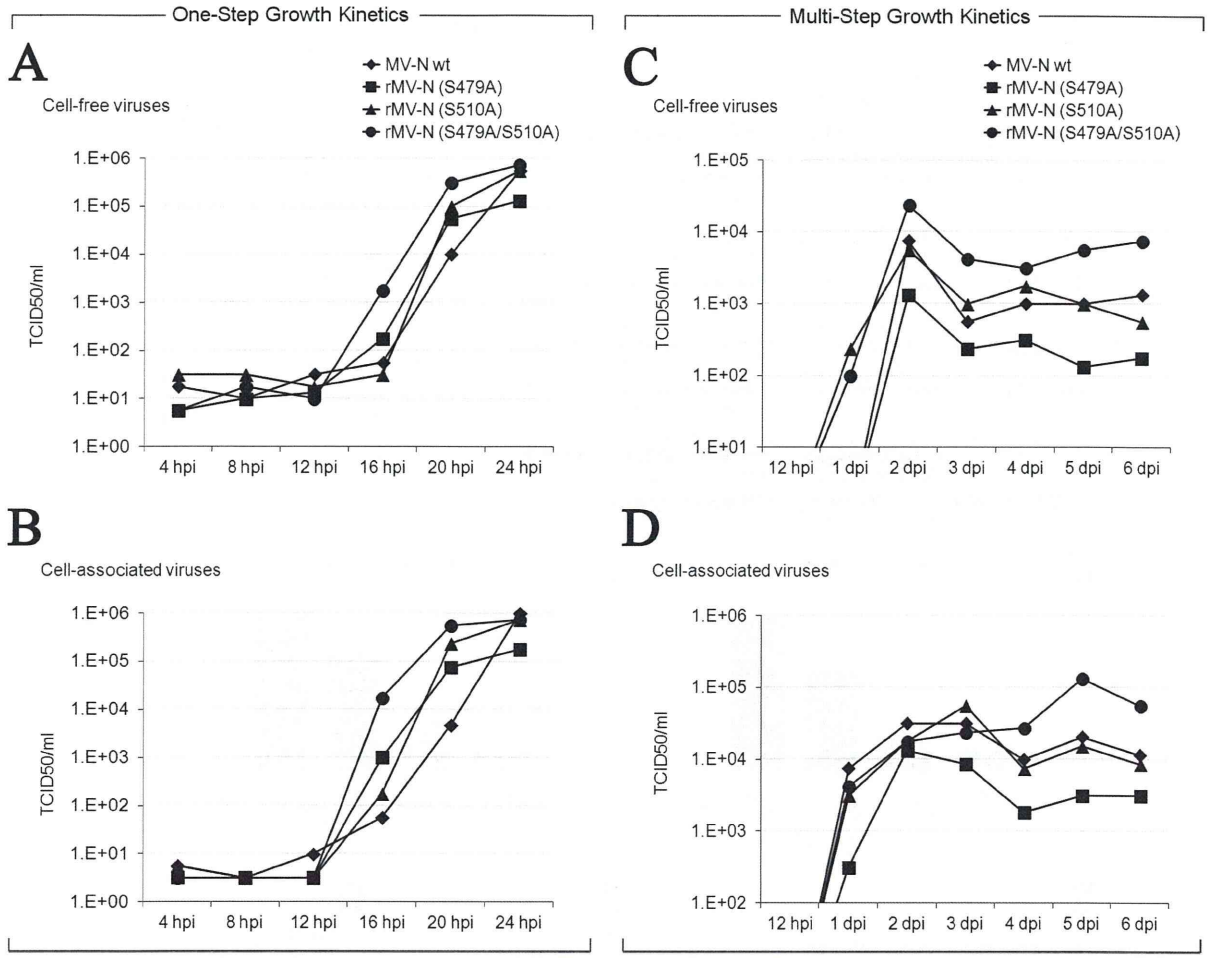

FIG 3 One- and multistep growth kinetics of rMVs. (A and B) 293SLAM cells were infected with wt-MV or rMVs (rMV-S479A, rMV-S510A, and rMV-S479A/S510A) at an MOI of 1.0. Cells were harvested at 4, 8, 12, 16, 20, and 24 hpi, and titrations ($TCID_{50}$/ml) of the cell-free virus (A) and cell-associated virus (B) were conducted. (C and D) 293SLAM cells infected with the rMVs at an MOI of 0.001 were harvested at 12 hpi, 1 dpi, 2 dpi, 3 dpi, 4 dpi, 5 dpi, and 6 dpi, and the titers of cell-free virus (C) and cell-associated virus (D) were measured.

S510A were relatively stable compared with those of wt-MV or rMV-S510A (Fig. 6A). This suggested that the stability of an encapsidated RNA was affected by the phosphorylation status of the N protein. We further analyzed the relationship between the phosphorylation of the N protein and binding to the viral genome using a nuclease protection assay. In agreement with the results of the pulse-labeling experiments, the genomic RNA protection rate of S479A/S510A was highest, reaching 52.8%. In contrast, genomic RNAs coated with wt-N and S510A provided 30.2% and 33.4% protection, respectively. The protection rate of S479A was limited to 10.3% (Fig. 6B). The viral genome protection rate significantly correlated with viral titers during the plateau phase of multistep growth kinetics (for cell-associated virus, $R^2 = 0.66$, $P < 0.001$; for cell-free virus, $R^2 = 0.91$, $P < 0.001$) (Fig. 6C). The protection rate inversely correlated with the phosphorylation level of the N protein ($R^2 = 0.96$, $P < 0.001$) (Fig. 6D). These correlations also showed an exponential relationship similar to that shown in Fig. 4F and G, implying that the influence of N-phosphorylation on the plateau phase of multistep growth kinetics is a result of differences in the levels of stability of the viral genomic RNA. Collectively, the results show that the phosphorylation intensity of the N protein affects the stability of the viral genomic RNA and that the viral titer during late-phase infection strongly depends upon viral genome stability.

DISCUSSION

We have demonstrated that phosphorylation of the N protein affects viral gene expression and viral genomic RNA stability. It has been reported that the P protein has two distinct binding sites for the free N protein and the N-RNA complex (31), and the P protein is therefore thought to be a carrier that binds free N proteins for delivery to the nascent replicating viral N-RNA complex for efficient encapsidation (4, 32). It has also been reported that the P protein reduces nonspecific binding of the N protein to cellular RNA (4). Thus, the P protein seems to play important roles in supporting viral genome encapsidation; changes in the phosphorylation status of the N protein via N-P interactions may also be required for appropriate formation of the nucleocapsid. In rabies virus, it has been reported that the phosphorylation level of the N protein associated with the P protein is kept low to strengthen its affinity for viral RNA (26, 33, 34). Consistent with these findings, we demonstrated significantly less phosphoryla-

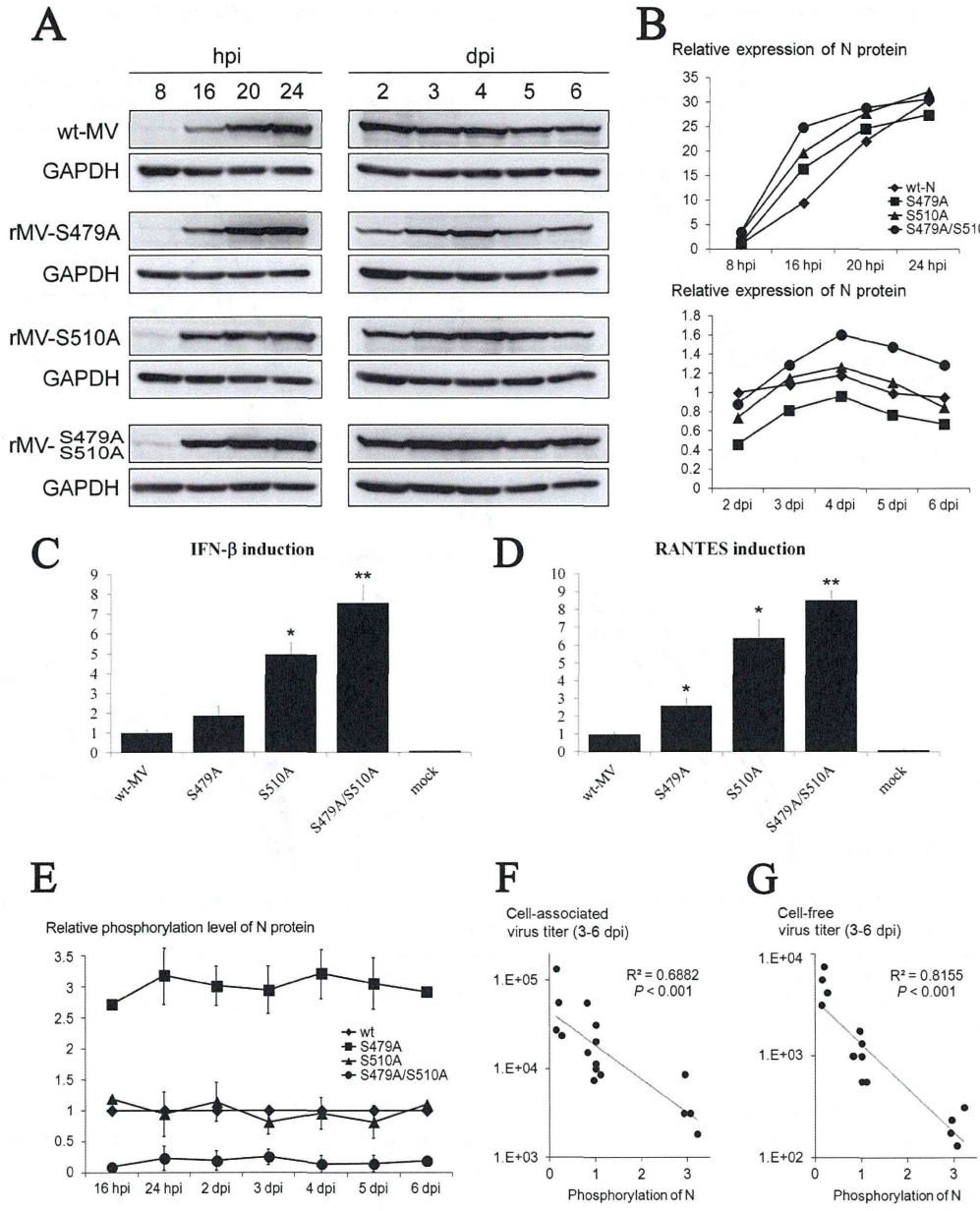

FIG 4 Viral N protein accumulation of wt-MV and rMVs and their phosphorylation statuses. (A) 293SLAM cells were infected with wt-MV and rMVs (rMV-S479A, rMV-S510A, and rMV-S479A/S510A) and lysed at 8, 16, 20, and 24 hpi (MOI = 1.0) or at 2, 3, 4, 5, and 6 dpi (MOI = 0.001). Lysates were subjected to 10% SDS-PAGE and immunoblotting with an anti-N polyclonal antibody. (B) Relative expression levels (nucleoprotein/GAPDH) of wt-N and phosphorylation mutants of the N protein. (C and D) IFN-β induction (C) and RANTES induction (D) by wt-MV and rMVs. *, $P < 0.05$; **, $P < 0.01$. (E) Relative phosphorylation levels of wt-N and N mutants in 293SLAM cells at each time point. (F and G) Correlation between phosphorylation level of the N protein and plateau-phase viral titers (3 to 6 dpi) during multistep growth kinetics (cell-free [G] and cell-associated [F] virus). R^2, coefficient of determination; *P*, *P* value.

tion of the wt-N protein associated with the P protein compared with that seen with the highly phosphorylated wt-N protein expressed on its own (Fig. 2). Hence, the P protein functions as a carrier of the N protein and seems to maintain the N protein at a lower phosphorylation state for effective encapsidation of the viral genome.

In the one-step growth experiments using rMVs, the phosphorylation of the N protein affected viral growth kinetics. The wt-MV showed delayed growth kinetics compared with the rMVs (Fig. 3A and B). The viral titer and N protein level for the wt-MV were similarly attenuated during the early growth phase until 24 hpi (Fig. 3A and B and 4A and B). This delay in wt-MV growth can be attributed to downregulation of viral gene expression. These results are not consistent with those we have previously reported. We demonstrated that mutations of the N-phosphorylation sites (S479A, S510A, and S479A/S510A) caused downregulation of viral transcription in a minigenome assay (16, 17). As with our data, some past reports that investigated the function of viral protein

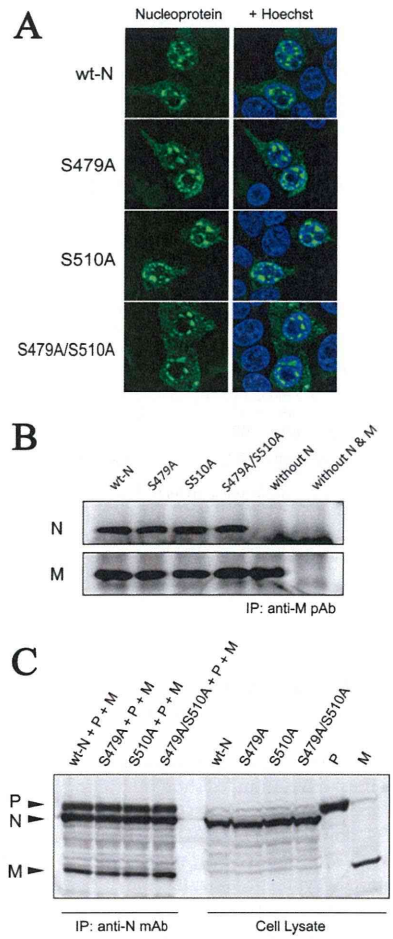

FIG 5 Nucleocytoplasmic trafficking and N-M protein interaction are not regulated by N-phosphorylation. (A) HEK293 cells were transfected with vectors encoding wt or N protein mutants. Locations of N proteins were visualized using an anti-N antibody. Nuclei were stained with Hoechst 33342. (B) Transiently expressed N protein and its phosphorylation mutants (S479A, S510A, and S479A/S510A) complexed with the M protein in HEK293 cells were coimmunoprecipitated with an anti-M polyclonal antibody. Precipitated N and M proteins were detected with anti-N and anti-M polyclonal antibodies, respectively. (C) HEK293 cells were transfected with plasmids encoding the N, P, and M proteins. Expressed proteins were precipitated with anti-N monoclonal antibody and detected by immunoblotting using anti-N, -P, and -M polyclonal antibodies.

phosphorylations have suggested these kinds of discrepancies between viral transcriptional activity and growth; mutations at constitutive phosphorylation sites of the human respiratory syncytial virus (RSV) P protein (232A/237A and 116L/117R/119L/232A/237A) did not have a significant impact on viral transcription and replication in a minigenome assay, while recombinant viruses with mutated phosphorylation sites (rA2-PP2 and rA2-PP5) showed significantly reduced growth kinetics compared with wild-type virus (35). High-turnover phosphorylation at S54 was dispensable for viral RNA synthesis and formation of N-P and P-L protein complexes in transfection experiments (36), whereas an absence of S54 phosphorylation caused attenuation of viral titers because the S54 phosphorylation is involved in the viral uncoating step (37). Thus, in functional analysis of viral protein phosphorylation, since it affects various steps of viral life cycle, viral infection experiments sometime show different results from transfection experiments.

Past reports have demonstrated that strategic regulation of RNA synthesis is required for effective evasion of the host defense system (38, 39, 40, 41). Likewise, we hypothesized that wt-MV strategically downregulated viral gene expression to evade the host defense system during the early phases of infection. It has been reported that transcription of the MV N gene causes cytokine induction in a dose- and time-dependent manner (28). Additionally, inhibition of viral transcription by limited UV irradiation or ribavirin treatment reduced MV-induced expression of cytokines, such as RANTES (CCL5) (28, 42), which is thought to play an important role in response to virus infection by recruiting monocytes, macrophages, and virus-specific memory T cells (41, 43, 44, 45, 46). It was also reported that uncontrolled rapid viral RNA synthesis induces cell death and expression of cytokines such as beta interferon and interleukin-6 (39). Thus, a negative regulatory system of viral RNA production has been reported in some viruses (39, 47). We demonstrated that attenuation of wt-MV viral gene expression activity during early growth phases contributed to reduced host immune responses (Fig. 4C and D). This feature of wt-MV could be advantageous in the context of real virus infections.

On the other hand, the differences in the plateau phase of multistep growth kinetics were inversely correlated with the phosphorylation intensity of the N protein (Fig. 3C and D and 4E). Reductions in the phosphorylation level of the N protein enhanced stability of encapsidated viral genomic RNA (Fig. 6A and B). These data indicate that virus growth in the plateau phase is affected by the stability of the encapsidated viral genomic RNA, which is in contrast to the early phases of infection. It has been previously reported that dephosphorylation of the N protein increases viral RNA encapsidation of the N protein in rabies virus (48). Moreover, removal of the C-terminal tail of the N protein, which contains major phosphorylation sites, makes the nucleocapsid more rigid in MV (49). These data suggest that the negatively charged N protein and the viral genomic RNA repel each other and that this electrostatic repulsion weakens encapsidation of the viral genome. Therefore, excessive phosphorylation of the N protein interferes with the rapid assembly and/or strong association of the N-RNA complex. During one-step growth kinetics, the total phosphorylation intensity of the N protein and viral genome stability do not have a strong impact on virus production (Fig. 3A and B). During an MV infection, the genomic RNA mainly replicates at around 12 to 24 hpi and accumulates exponentially during this phase (50). Because an adequate amount of genomic RNA was supplied during this phase, viral RNA stability does not have a strong influence during the early phases of infection. In contrast, viral genome replication is restricted to the latter phases of infection. Hence, viral genome stability has a strong selective effect on the late phase of multistep growth kinetics.

In the present study, we demonstrated that N-phosphorylation affected viral growth by altering viral gene expression and genomic RNA stability. However, we also observed that nucleocytoplasmic transport of the N protein (Fig. 5A), N-P interactions (Fig. 1B and 5C), and N-M interactions (Fig. 5B and C) remained unaltered. During the early phases of infection, proper phosphorylation of the N protein controls viral gene expression, and this regulation was required for efficient evasion of the host immune response. The phosphorylation intensity of the N protein at pla-

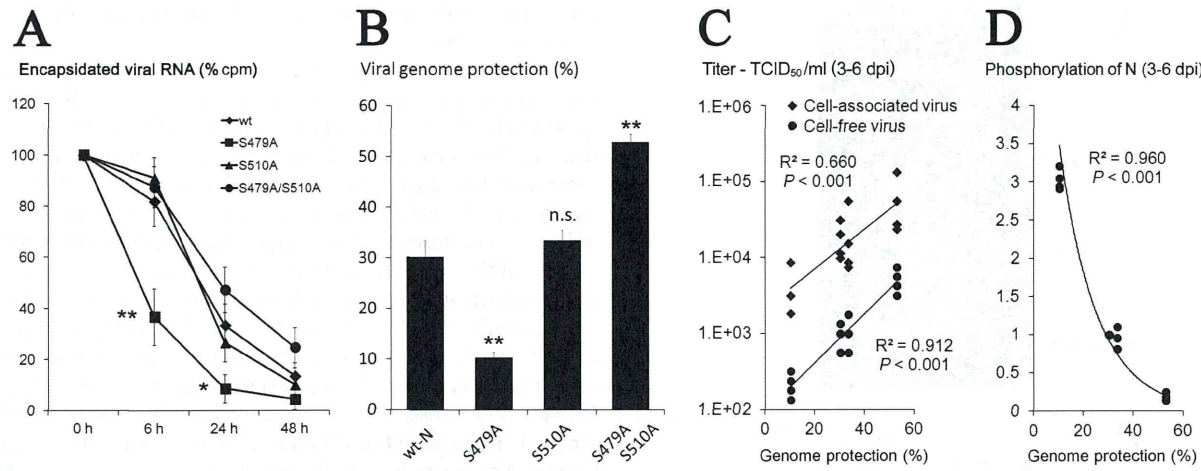

FIG 6 Phosphorylation intensity of the N protein inversely correlated with viral genome stability. (A) 293SLAM cells were infected with wt-MV or rMVs (S479A, S510A, and S479A/S510A) at an MOI of 0.01. Infected cells were pulse-chased with tritium. Cells and supernatants were collected at 0, 6, 24, and 48 h after labeling, and radioactivity was measured. (B) 293SLAM cells were infected with wt-MV or rMVs, and each N-RNA complex in the cell lysate was treated with MNase. Viral genomic RNAs of MNase-treated samples or untreated samples were quantified by RT-PCR. Error bars indicate standard deviations. **, $P < 0.01$; n.s., not significant. (C) Correlation between viral genome protection rate and viral growth of wt or mutant MVs. (D) Viral genome protection rate and the phosphorylation level of N proteins.

teau growth phases regulates viral genome stability, and these data provide new insights into the machinery regulating postreplication viral RNAs. The N protein may regulate its own phosphorylation (S479 and S510), thereby optimizing its function at each step of the viral life cycle for efficient viral propagation. Further analysis of the phosphorylation and dephosphorylation mechanisms of the N protein would help our understanding of the biological significance of N protein phosphorylation regulation.

ACKNOWLEDGMENT

This study was supported by Grants-in-Aid from the Ministry of Education, Culture, Sports, Science and Technology, Japan.

REFERENCES

1. **Wolfson LJ, Strebel PM, Gacic-Dobo M, Hoekstra EJ, McFarland JW, Hersh BS; Measles Initiative.** 2007. Has the 2005 measles mortality reduction goal been achieved? A natural history modelling study. Lancet **369**:191–200.
2. **Ray J, Fujinami RS.** 1987. Characterization of in vitro transcription and transcriptional products of measles virus. J. Virol. **61**:3381–3387.
3. **Cevik B, Holmes DE, Vrotsos E, Feller JA, Smallwood S, Moyer SA.** 2004. The phosphoprotein (P) and L binding sites reside in the N-terminus of the L subunit of the measles virus RNA polymerase. Virology **327**: 297–306.
4. **Curran J.** 1996. Reexamination of the Sendai virus P protein domains required for RNA synthesis: a possible supplemental role for the P protein. Virology **221**:130–140.
5. **Harrison MS, Sakaguchi T, Schmitt AP.** 2010. Paramyxovirus assembly and budding: building particles that transmit infections. Int. J. Biochem. Cell Biol. **42**:1416–1429.
6. **Vincent S, Gerlier D, Manie SN.** 2000. Measles virus assembly within membrane rafts. J. Virol. **74**:9911–9915.
7. **Hashiguchi T, Maenaka K, Yanagi Y.** 2011. Measles virus hemagglutinin: structural insights into cell entry and measles vaccine. Front. Microbiol. **2**:247.
8. **Bhella D, Ralph A, Yeo RP.** 2004. Conformational flexibility in recombinant measles virus nucleocapsids visualised by cryo-negative stain electron microscopy and real-space helical reconstruction. J. Mol. Biol. **340**: 319–331.
9. **Lund GA, Tyrrell DL, Bradley RD, Scraba DG.** 1984. The molecular length of measles virus RNA and the structural organization of measles nucleocapsids. J. Gen. Virol. **65**(Pt 9):1535–1542.
10. **Calain P, Roux L.** 1993. The rule of six, a basic feature for efficient replication of Sendai virus defective interfering RNA. J. Virol. **67**:4822–4830.
11. **Bitko V, Barik S.** 2001. Phenotypic silencing of cytoplasmic genes using sequence-specific double-stranded short interfering RNA and its application in the reverse genetics of wild type negative-strand RNA viruses. BMC Microbiol. **1**:34. doi:10.1186/1471-2180-1-34.
12. **Moyer SA, Smallwood-Kentro S, Haddad A, Prevec L.** 1991. Assembly and transcription of synthetic vesicular stomatitis virus nucleocapsids. J. Virol. **65**:2170–2178.
13. **Rima BK, Duprex WP.** 2009. The measles virus replication cycle. Curr. Top. Microbiol. Immunol. **329**:77–102.
14. **Thorne HV, Dermott E.** 1977. Y-forms as possible intermediates in the replication of measles virus nucleocapsids. Nature **268**:345–347.
15. **Kolakofsky D, Le Mercier P, Iseni F, Garcin D.** 2004. Viral DNA polymerase scanning and the gymnastics of Sendai virus RNA synthesis. Virology **318**:463–473.
16. **Hagiwara K, Sato H, Inoue Y, Watanabe A, Yoneda M, Ikeda F, Fujita K, Fukuda H, Takamura C, Kozuka-Hata H, Oyama M, Sugano S, Ohmi S, Kai C.** 2008. Phosphorylation of measles virus nucleoprotein upregulates the transcriptional activity of minigenomic RNA. Proteomics **8**:1871–1879.
17. **Sugai A, Sato H, Yoneda M, Kai C.** 2012. Phosphorylation of measles virus phosphoprotein at S86 and/or S151 downregulates viral transcriptional activity. FEBS Lett. **586**:3900–3907.
18. **Kobune F, Takahashi H, Terao K, Ohkawa T, Ami Y, Suzaki Y, Nagata N, Sakata H, Yamanouchi K, Kai C.** 1996. Nonhuman primate models of measles. Lab. Anim. Sci. **46**:315–320.
19. **Terao-Muto Y, Yoneda M, Seki T, Watanabe A, Tsukiyama-Kohara K, Fujita K, Kai C.** 2008. Heparin-like glycosaminoglycans prevent the infection of measles virus in SLAM-negative cell lines. Antiviral Res. **80**:370–376.
20. **Kai C, Ochikubo F, Okita M, Iinuma T, Mikami T, Kobune F, Yamanouchi K.** 1993. Use of B95a cells for isolation of canine distemper virus from clinical cases. J. Vet. Med. Sci. **55**:1067–1070.
21. **Kobune F, Sakata H, Sugiura A.** 1990. Marmoset lymphoblastoid cells as a sensitive host for isolation of measles virus. J. Virol. **64**:700–705.
22. **Sato H, Honma R, Yoneda M, Miura R, Tsukiyama-Kohara K, Ikeda F, Seki T, Watanabe S, Kai C.** 2008. Measles virus induces cell-type specific changes in gene expression. Virology **375**:321–330.
23. **Tatsuo H, Ono N, Tanaka K, Yanagi Y.** 2000. SLAM (CDw150) is a cellular receptor for measles virus. Nature **406**:893–897.
24. **Niwa H, Yamamura K, Miyazaki J.** 1991. Efficient selection for high-

expression transfectants with a novel eukaryotic vector. Gene **108**:193–199.
25. **Masuda M, Sato H, Kamata H, Katsuo T, Takenaka A, Miura R, Yoneda M, Tsukiyama-Kohara K, Mizumoto K, Kai C.** 2006. Characterization of monoclonal antibodies directed against the canine distemper virus nucleocapsid protein. Comp. Immunol. Microbiol. Infect. Dis. **29**:157–165.
26. **Huber M, Cattaneo R, Spielhofer P, Orvell C, Norrby E, Messerli M, Perriard JC, Billeter MA.** 1991. Measles virus phosphoprotein retains the nucleocapsid protein in the cytoplasm. Virology **185**:299–308.
27. **Sato H, Masuda M, Miura R, Yoneda M, Kai C.** 2006. Morbillivirus nucleoprotein possesses a novel nuclear localization signal and a CRM1-independent nuclear export signal. Virology **352**:121–130.
28. **Noe KH, Cenciarelli C, Moyer SA, Rota PA, Shin ML.** 1999. Requirements for measles virus induction of RANTES chemokine in human astrocytoma-derived U373 cells. J. Virol. **73**:3117–3124.
29. **Bernard C, Gely S, Bourhis JM, Morelli X, Longhi S, Darbon H.** 2009. Interaction between the C-terminal domains of N and P proteins of measles virus investigated by NMR. FEBS Lett. **583**:1084–1089.
30. **Iwasaki M, Takeda M, Shirogane Y, Nakatsu Y, Nakamura T, Yanagi Y.** 2009. The matrix protein of measles virus regulates viral RNA synthesis and assembly by interacting with the nucleocapsid protein. J. Virol. **83**: 10374–10383.
31. **Karlin D, Ferron F, Canard B, Longhi S.** 2003. Structural disorder and modular organization in Paramyxovirinae N and P. J. Gen. Virol. **84**(Pt 12):3239–3252.
32. **Leyrat C, Yabukarski F, Tarbouriech N, Ribeiro EA, Jr, Jensen MR, Blackledge M, Ruigrok RW, Jamin M.** 2011. Structure of the vesicular stomatitis virus N^0P complex. PLoS Pathog. **7**:e1002248. doi:10.1371/journal.ppat.1002248.
33. **Wu X, Gong X, Foley HD, Schnell MJ, Fu ZF.** 2002. Both viral transcription and replication are reduced when the rabies virus nucleoprotein is not phosphorylated. J. Virol. **76**:4153–4161.
34. **Kawai A, Toriumi H, Tochikura TS, Takahashi T, Honda Y, Morimoto K.** 1999. Nucleocapsid formation and/or subsequent conformational change of rabies virus nucleoprotein (N) is a prerequisite step for acquiring the phosphatase-sensitive epitope of monoclonal antibody 5-2-26. Virology **263**:395–407.
35. **Lu B, Ma CH, Brazas R, Jin H.** 2002. The major phosphorylation sites of the respiratory syncytial virus phosphoprotein are dispensable for virus replication in vitro. J. Virol. **76**:10776–10784.
36. **Asenjo A, Rodríguez L, Villanueva N.** 2005. Determination of phosphorylated residues from human respiratory syncytial virus P protein that are dynamically dephosphorylated by cellular phosphatases: a possible role for serine 54. J. Gen. Virol. **86**(Pt 4):1109–1120.
37. **Asenjo A, González-Armas JC, Villanueva N.** 2008. Phosphorylation of human respiratory syncytial virus P protein at serine 54 regulates viral uncoating. Virology **380**:26–33.
38. **Gainey MD, Dillon PJ, Clark KM, Manuse MJ, Parks GD.** 2008. Paramyxovirus-induced shutoff of host and viral protein synthesis: role of the P and V proteins in limiting PKR activation. J. Virol. **82**:828–839.
39. **Sun D, Luthra P, Li Z, He B.** 2009. PLK1 down-regulates parainfluenza virus 5 gene expression. PLoS Pathog. **5**:e1000525. doi:10.1371/journal.ppat.1000525.
40. **Fuentes SM, Sun D, Schmitt AP, He B.** 2010. Phosphorylation of paramyxovirus phosphoprotein and its role in viral gene expression. Future Microbiol. **5**:9–13.
41. **Dillon PJ, Parks GD.** 2007. A role for the P subunit of the paramyxovirus polymerase in limiting host cell antiviral responses. J. Virol. **81**:11116–11127.
42. **Schall TJ, Jongstra J, Dyer BJ, Jorgensen J, Clayberger C, Davis MM, Krensky AM.** 1988. A human T cell-specific molecule is a member of a new gene family. J. Immunol. **141**:1018–1025.
43. **Nakamichi K, Saiki M, Sawada M, Takayama-Ito M, Yamamuro Y, Morimoto K, Kurane I.** 2005. Rabies virus-induced activation of mitogen-activated protein kinase and NF-kappaB signaling pathways regulates expression of CXC and CC chemokine ligands in microglia. J. Virol. **79**: 11801–11812.
44. **Pazdrak K, Olszewska-Pazdrak B, Liu T, Takizawa R, Brasier AR, Garofalo RP, Casola A.** 2002. MAPK activation is involved in posttranscriptional regulation of RSV-induced RANTES gene expression. Am. J. Physiol. Lung Cell Mol. Physiol. **283**:L364–L372.
45. **Kujime K, Hashimoto S, Gon Y, Shimizu K, Horie T.** 2000. p38 mitogen-activated protein kinase and c-jun-NH2-terminal kinase regulate RANTES production by influenza virus-infected human bronchial epithelial cells. J. Immunol. **164**:3222–3228.
46. **Schall TJ, Bacon K, Toy KJ, Goeddel DV.** 1990. Selective attraction of monocytes and T lymphocytes of the memory phenotype by cytokine RANTES. Nature **347**:669–671.
47. **Schmid S, Metz P, Prat CM, Gonzalez-Dunia D, Schwemmle M.** 2010. Protein kinase C-dependent phosphorylation of Borna disease virus P protein is required for efficient viral spread. Arch. Virol. **155**:789–793.
48. **Yang J, Koprowski H, Dietzschold B, Fu ZF.** 1999. Phosphorylation of rabies virus nucleoprotein regulates viral RNA transcription and replication by modulating leader RNA encapsidation. J. Virol. **73**:1661–1664.
49. **Schoehn G, Mavrakis M, Albertini A, Wade R, Hoenger A, Ruigrok RW.** 2004. The 12 A structure of trypsin-treated measles virus N-RNA. J. Mol. Biol. **339**:301–312.
50. **Plumet S, Duprex WP, Gerlier D.** 2005. Dynamics of viral RNA synthesis during measles virus infection. J. Virol. **79**:6900–6908.

OPEN ACCESS Freely available online

PLOS ONE

Recombinant Measles Virus Vaccine Expressing the Nipah Virus Glycoprotein Protects against Lethal Nipah Virus Challenge

Misako Yoneda[1]*, Marie-Claude Georges-Courbot[3], Fusako Ikeda[1], Miho Ishii[1], Noriyo Nagata[4], Frederic Jacquot[3], Hervé Raoul[3], Hiroki Sato[1], Chieko Kai[1,2]*

1 Laboratory Animal Research Center, Institute of Medical Science, The University of Tokyo, Minato-ku, Tokyo, Japan, **2** International Research Center for Infectious Diseases, Institute of Medical Science, The University of Tokyo, Minato-ku, Tokyo, Japan, **3** Institut National de la Sante et de la Recherche Médicale, Laboratory P4 INSERM Jean Mérieux, Lyon, France, **4** National Institute of Infectious Diseases, Department of Pathology Tokyo, Japan

Abstract

Nipah virus (NiV) is a member of the genus *Henipavirus*, which emerged in Malaysia in 1998. In pigs, infection resulted in a predominantly non-lethal respiratory disease; however, infection in humans resulted in over 100 deaths. Nipah virus has continued to re-emerge in Bangladesh and India, and person-to-person transmission appeared in the outbreak. Although a number of NiV vaccine studies have been reported, there are currently no vaccines or treatments licensed for human use. In this study, we have developed a recombinant measles virus (rMV) vaccine expressing NiV envelope glycoproteins (rMV-HL-G and rMV-Ed-G). Vaccinated hamsters were completely protected against NiV challenge, while the mortality of unvaccinated control hamsters was 90%. We trialed our vaccine in a non-human primate model, African green monkeys. Upon intraperitoneal infection with NiV, monkeys showed several clinical signs of disease including severe depression, reduced ability to move and decreased food ingestion and died at 7 days post infection (dpi). Intranasal and oral inoculation induced similar clinical illness in monkeys, evident around 9 dpi, and resulted in a moribund stage around 14 dpi. Two monkeys immunized subcutaneously with rMV-Ed-G showed no clinical illness prior to euthanasia after challenge with NiV. Viral RNA was not detected in any organ samples collected from vaccinated monkeys, and no pathological changes were found upon histopathological examination. From our findings, we propose that rMV-NiV-G is an appropriate NiV vaccine candidate for use in humans.

Citation: Yoneda M, Georges-Courbot M-C, Ikeda F, Ishii M, Nagata N, et al. (2013) Recombinant Measles Virus Vaccine Expressing the Nipah Virus Glycoprotein Protects against Lethal Nipah Virus Challenge. PLoS ONE 8(3): e58414. doi:10.1371/journal.pone.0058414

Editor: Maria G. Masucci, Karolinska Institutet, Sweden

Received October 4, 2012; **Accepted** February 4, 2013; **Published** March 14, 2013

Funding: This work was supported by grants in aid from the Ministry of Education, Science, Culture and Sports of Japan. The funders had no role in study design, data collection and analysis, decision to publish, or preparation of the manuscript.

Competing Interests: The authors have declared that no competing interests exist.

* E-mail: yone@ims.u-tokyo.ac.jp (MY); ckai@ims.u-tokyo.ac.jp (CK)

Introduction

Nipah virus (NiV) is a member of the genus *Henipavirus*, within the family Paramyxoviridae. This virus emerged in Malaysia in 1998, resulting in predominantly nonlethal respiratory disease in pigs. However, in humans, there were 105 deaths. In the first outbreak, pigs were the amplifying host [1,2] and they were probably infected through fruits contaminated by secretions and/or body fluids from bats [3]. In Malaysia, a higher prevalence of infection was found among pig farmers, pork sellers and army personnel involved in the culling of pigs. However, person-to-person transmission was not apparent at the time. NiV has re-emerged in Bangladesh and India, with the total number of reprted cases exceeding 300, with 161 fatalities [4]. These new outbreaks have occured in patients who have never come in contact with pigs, therefore it is suspected that the infection is being directly transmitted from fruit bats, and person-to-person transmission has been noted in some cases in Bangladesh [5,6,7,8]. NiV infection causes a severe acute encephalitic syndrome or a severe respiratory disease with high mortality in humans [2,9–13]. Although many patients eventually recover fully, some develop neurological manifestations several months after recovery from acute non-encephalitic or asymptomatic infection. There are four countries where NiV outbreaks have occurred, or are currently in progress. The habitat of fruit bats, the natural hosts of NiV infection, is widely distributed in the world [4] from Australia, South-East and South Asia to west coast of Africa. To prevent further outbreaks, it is necessary that effective vaccines and therapies are developed.

A number of NiV vaccine studies have been conducted in which the NiV envelope proteins F (fusion) and G (glycoprotein), were chosen for vaccine development based on existing knowledge regarding immunity to other paramyxoviruses. Vaccinia virus-expressed recombinant NiV F and G proteins have been shown to be immunogenic, and can induce protective immune responses in hamsters [14]. Canarypox virus-based vaccine vectors carrying genes encoding NiV F or G proteins induce neutralizing antibodies in pigs and prevent viral shedding during NiV challenge [15]. However, there are currently no vaccines or treatments licensed for human use.

Our aim was to develop an affordable, live-attenuated MV vaccine that could be used in areas where NiV outbreaks are

occurring. MV-based vaccines induce life-long immunity after one or two low-dose inoculations [16–18]. The MV vector can stably express proteins derived from other infectious viruses, inducing strong and long-term humoral and cellular immune responses, even if there is preexisting immunity to MV [19–21].

In the present study, we evaluated whether African green monkeys were a suitable animal model for NiV infection. We also examined the efficacy of vaccination in the monkey model as well as a previously established hamster model, with recombinant MV vectors expressing the G protein of NiV.

Materials and Methods

Ethique

The majority of this work was performed in a biosafety level 4 (BSL4) laboratory at INSERM, Lyon, France and carried out in strict accordance with the French "Comité National de Réflexion Etihque sur l'Expérimentation Animale": All animal experiments were approved by Comité régional d'ethique pour l'expérimentation animale Rhone Alpes (Permit Number: 0236, 324, P4_2010_004). All surgery was performed under sodium pentobarbital anesthesia, and all efforts were made to minimize suffering.

Animals and Housing

African green monkeys (n = 8) were studied, then euthanized under anesthesia at the end of experimental period. Monkeys were individually housed in cages, and had free access to food and water. They were given pellet, fruits and confectionery once a day. During the experiment, toys such as mirrors, balls and rings especially designed for monkeys, were provided.

We also examined hamsters (n = 30), which were euthanized under anesthesia at the completion of the experiment.

Cells and Viruses

The NiV we used was propagated in Vero cells grown in Dulbecco's minimal essential medium (DMEM) supplemented with 5% fetal calf serum (FCS), L-glutamine, penicillin and streptomycin at 37°C/5% CO_2. Virus titration was conducted by assessing the 50% tissue culture infectious dose ($TCID_{50}$) in 96-well plates. To generate a recombinant MV (rMV) expressing the NiV G protein, we used replication competent MV-based vectors (pMV-HL, HL strain; pMV-Ed, Edmonston B strain) [22,23]. The NiV G cDNA was amplified from pNiV(6+) [24] by using following primers, NipG-SacI-F, 5′-*GAGCTC*ATGCCGGCAGAAAACAAGAA-3′ (SacI site in italic); and reverse primer NipG-FseI-R 5′-*GGCCGGCC***TA**TTATGTACATTGCTCTGGTA-3′ (FseI site in italics; additional two nucleotides for rule of six in boldface). The intergenic region between the N and P junction was amplified by using the following primers. NP-F, *GGCCGGCC*TCCAATATTCTA (FseI site in italics); and reverse primer NP-R, *GAGCTC*CATTGGATGAATTGTTATTA (SacI site in italics). The PCR products were cloned into pGEM-T Easy (Promega, Madison, WI, USA). The NiV G fragment was inserted downstream of the N-P intergenic region, followed by digestion by SacI. Finally, the fragment of NiV G connected to the N-P intergenic region was cloned into the FseI site of the pMV-HL and pMV-Ed, and the resulting clones were used to rescue the infectious recombinant MVs expressing NiV G protein (rMV-HL-G and rMV-Ed-G).

NiV Infection of African Green Monkeys

Young adult African green monkeys (Chlorocebus aethiops; n = 4), weighing 4–5 kg were caged individually. All animals were anesthetized and inoculated with 1×10^6 or 1×10^8 $TCID_{50}$ of NiV by intraperitoneal or intranasal and per os routes. Animals were anesthetized for clinical examination, temperature, weight, blood draws and nasal and oral swabs on days 0, 2, 4, 7, 9, 11, 14, 16, 18, 21, 24. Animals were sacrificed when they reached a moribund state, or showed symptoms of irreversible disease (15% weight loss, or no intake of food and water).

Immunization and Challenge

For protection studies, 10 8-week-old golden hamsters were immunized intraperitoneally with 2×10^4 $TCID_{50}$ of the recombinant MVs at 0 and 21 dpi. Hamsters were challenged 1 week after the second immunization. Two African green monkeys were immunized subcutaneously with 1×10^5 $TCID_{50}$ of the recombinant MV-Ed-G on 0 and 28 dpi. Monkeys were challenged 2 weeks after the second immunization.

Measurement of Antibody Titres

The titer of antibodies against the NiV G protein (anti-NiV G) in the monkey sera was determined using an indirect enzyme-linked immunosorbent assay (ELISA). Ninety-six-well microtitre plates were coated with a 2 µg/ml solution of purified NiV G protein diluted in coating buffer (0.1 M carbonate-hydrogen carbonate buffer, pH9.6) overnight. Unoccupied sites in wells were blocked with 300 µl of 0.8% Block Ace (Dainihonseiyaku, Osaka, Japan) in PBS at room temperature for 3 h, washed with PBS containing 0.05% Tween 20 (PBS-T). Monkey sera (100 µL) were serially diluted 2-fold (1:100 to 1:12800) and added to duplicate wells. After 2 h incubation at 4°C, the wells were washed with PBS-T and incubated for 1 h with 100 µl of horseradish peroxidase (HRP)-conjugated goat anti-monkey-IgG (1:1000 dilution; CAPPEL). Following a final wash with PBS-T, 100 µl of peroxidase substrate (Bio-Rad Laboratories) was added to each well and the absorbance at 655 nm measured 30 min later.

Quantitative Real-time PCR (qPCR) Analyses

Tissue and swab samples were homogenized in 500 µl of Trizol reagent (Ambion) and total RNA extracted in accordance with the instructions of the manufacturer. First strand cDNA was synthesized using total RNA and random primers. The qPCR assays were carried out on an ABI Prism 7900HT (Applied Biosystems, USA) using SYBR Premix Ex TaqII (Takara, Japan). Specific Ribosomal Protein L13A (RPL13A) was used as an internal control. Data were analyzed with Sequence Detection Systems version 1.7a software (Applied Biosystems). Expression levels of the target genes were calculated using the threshold cycle time (Ct), the first cycle number at which emitted fluorescence exceeds 10X the standard deviation (SD) of base-line emission as measured in the cycles of PCR. A standard curve was generated using known cDNA concentrations (10-fold dilution from 10 ng ~ 1 pg/reaction). Normalized results were expressed as the ratio of NiV N RNA to RPL13A RNA.

Histopathological Examination

Tissues were processed by routine histological methods and sections of tissue were stained with hematoxylin and eosin and examined for histopathological changes. Separate sections were stained using immunohistochemical techniques with a rabbit polyclonal antiserum against the NiV nucleoprotein.

Results

rMV Vaccine Expressing the NiV G Protein

Recombinant viruses expressing the NiV G protein were generated and rescued using vectors based on the HL (pMV-HL) and Edmonston (pMV-Ed) strains [22,23]. The rescued viruses were tested for the expression of G protein using infected cells. B95a and Vero cells were infected with the rMVs (rMVs, rMV-HL-G and rMV-Ed-G) and the expression of NiV G was examined by immunofluorescence. The NiV G protein was well expressed in rMV-HL-G- or rMV-Ed-G-infected cells (Fig. 1A). We compared the *in vitro* growth characteristics of the recombinant viruses with those of the parental virus (Fig. 1B). rMV-HL-G grew well and had a growth rate similar to that of the parental rMV-HL virus. In contrast, the rMV-Ed-G had lower maximum titers than its parental virus. The sequence of the inserted NiV G gene in recovered viruses was checked and no substitutions were observed.

Vaccination of Hamsters with rMV Expressing NiV G Protects against a Lethal Infection

Hamsters are not fully susceptible to MV infection, but are highly susceptible to NiV infection. In our preliminary experiments, antibodies against MV were observed to increase in the sera from hamsters 3 weeks after intraperitoneal inoculation with MV, although the hamsters did not exhibit any symptoms of infection. In the present study, 8-week-old golden hamsters were intraperitoneally immunized with 2×10^4 $TCID_{50}$ of rMV-HL-G or rMV-Ed-G. Three weeks later, antibodies against NiV G, as measured by ELISA, were observed in the sera of all animals inoculated with rMV-HL-G (1:400), and in most of animals except one with rMV-Ed-G. All the animals were boosted with the same dose of the rMVs and then challenged 1 week after the second immunization. The ELISA titer was expressed as reciprocal of the dilution factor. Serum antibody titers increased in all hamsters well; in 9 rMV-HL-G-vaccinated hamsters; >1:1600 and in 1; 1:800, and in 9 rMV-Ed-G vaccinated hamsters; >1:1600 and 1; 1:200 at the challenge day. In the NiV hamster model, intraperitoneal inoculation of NiV induces fatal encephalitis 7 to 10 days later [24,25]. When unimmunized control hamsters were challenged intraperitoneally with 10^3 $TCID_{50}$/animal of NiV, 90% died (Fig. 2). However, all hamsters vaccinated with rMV-HL-G or rMV-Ed-G showed complete protection. During the observation period (14 days after the challenge), all hamsters immunized with the recombinant MVs showed no clinical symptoms of the disease and survived.

Nipah Virus Infection in African Green Monkeys

Intraperitoneal inoculation of one monkey with 1×10^6 $TCID_{50}$ NiV and one monkey with 1×10^8 $TCID_{50}$ NiV resulted in death within 7 days. Body weights began to decrease by 2 dpi (Fig. 3), and clinical signs including severe depression, reduced ability to move, and reduced food ingestion were observed from 5 dpi. Inoculation with NiV by intranasal and oral routes was also tested in the monkeys, to mimic natural infection in humans. Although a combined intranasal and oral inoculation was not lethal for monkeys, it caused similar clinical illness beginning at 9 dpi, and progressed at a slower rate than when the intraperitoneal route was used. Monkeys were seriously moribund at around 14 dpi. In particular, the monkey inoculated with 1×10^8 $TCID_{50}$ of virus by the intranasal and oral route lost 10% of its weight in 14 days. The monkey inoculated with 1×10^6 $TCID_{50}$ NiV by the same route lost 6% of its weight in 14 days. Blood biochemistry results for both monkeys showed an increase in both the total number of white blood cells and the lymphocyte/monocyte ratio by around 14 dpi (data not shown).

To assess the extent of NiV replication and tissue tropism in monkeys, the relative quantity of NiV RNA was measured in swabs and tissue samples. In the monkeys inoculated with NiV intraperitoneally and euthanized at 7 dpi, viral RNA was detected at variable levels in the tissues of many organs (Fig. 4). The highest relative levels of viral RNA were detected in the lung tissue of the monkey inoculated with 1×10^8 $TCID_{50}$ NiV, and in the spleen of monkey inoculated with 1×10^6 $TCID_{50}$ NiV. Viral RNA was not detected in tissues from monkeys inoculated with NiV by intranasal and oral routes. These monkeys had recovered from infection and were euthanized at 24 dpi for tissue collection.

Histopathological changes observed in the infected monkeys are shown in Table 1. In the monkeys inoculated with NiV intraperitoneally, advanced lesions were found in many abdominal organs and the lungs. Confluent consolidations with serum protein in lung alveoli and pulmonary congestion with edema were observed in both monkeys inoculated by the intraperitoneal route. In their spleen, severe hemorrhage, necrosis and lyphocyte depletion were oserved. These histopathological changes were similar to those observed in human cases. Virus antigen was also observed in vascular endothelial cells of small vein and capillaries in the lung, and in the follicular area in spleen. In monkeys inoculated with NiV *via* the intranasal and oral routes and euthanized at 24 dpi, follicular hyperplasia was seen in the spleens and tonsils of both monkeys. However, severe pathological changes in lung were observed only in the monkey inoculated with 1×10^8 $TCID_{50}$ NiV. There were no apparent changes in brain samples from of any of the monkeys.

Application of the rMV Vaccines for Monkeys

Two monkeys were subcutaneously immunized with 1×10^5 $TCID_{50}$ rMV-Ed-G. Four weeks later, they were boosted with the same dose of rMV-Ed-G. The vaccinations well induced antibody responses against NiV G protein. One monkey showed antibody response at 14 dpi, and both monkeys showed high serum antibody titers 1 week after the second immunization (Table 2). The vaccinated and unvaccinated monkeys were challenged intropertoneally with 1×10^5 $TCID_{50}$ NiV 1 week after the second immunization. The unvaccinated monkeys showed a decrease in rectal temperature 13 days after challenge, and clinical signs of illness; this was not observed in the vaccinated monkeys (Fig. 5). The vaccinated monkeys did not show any clinical illness prior to euthanasia. Their organ samples, taken 21 days after NiV challenge, were tested for presence of viral RNA by qPCR. Viral RNA was detected only in the brain and liver of an unvaccinated monkey (T+ SV085).

We also examined these monkeys for histophathological changes. In the lungs of unvaccinated monkeys, severe congestion was widely observed in addition to the accumulation of blood plasma in alveoli simiar to those with previous experiment (Fig. 6). Perivascular edema and lymphocytic infiltration around vessels were also observed. In the brain, perivascular cuffing and an accumulation of glial and foam cells were observed in the cerebral cortex. There were no lesions observed in the tissues of vaccinated monkeys.

Discussion

NiV is a zoonotic virus that has recently emerged in Malaysia. It has a broad host range and can cause severe respiratory illness and encephalitis with high mortality in humans [26]. Despite several previous NiV vaccine studies, there are still no licensed vaccines

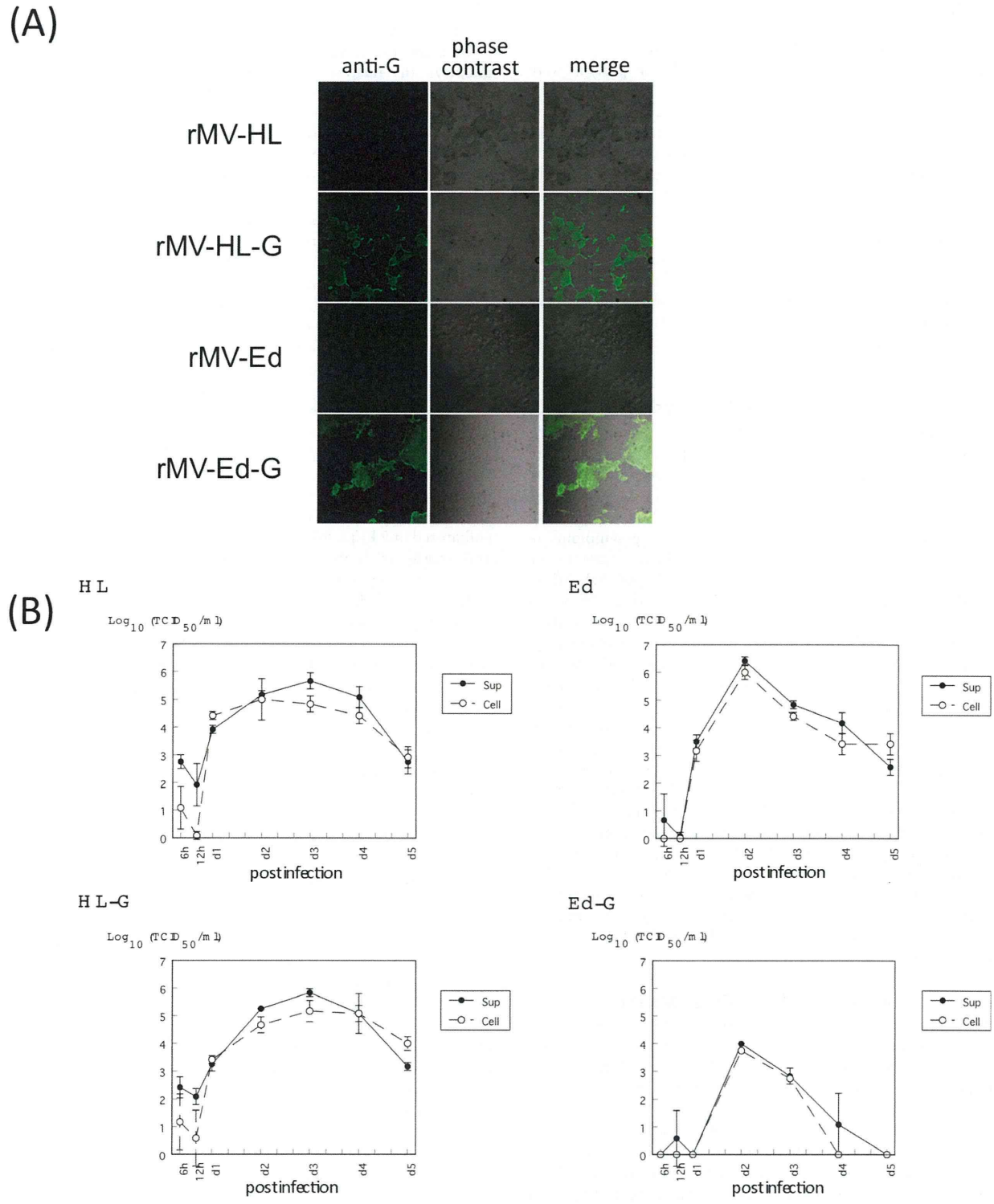

Figure 1. Recombinant measles virus expressing NiV G protein. Two strains of rMV expressing the NiV G protein were generated; rMV-HL-G and rMV-Ed-G. (A) rMV-HL-G-infected B95a cells and rMV-Ed-G-infected Vero cells were stained with anti-NiV G polyclonal antibody and analyzed by phase contrast microscopy and immunofluorescence. Cells infected with empty vectors served as controls. (B) B95a cells were infected with rMV-HL or rMV-HL-G. Vero cells were infected with rMV-Ed or rMV-Ed-G. Infections were conducted at a multiplicity of infection (MOI) of 0.1 $TCID_{50}$/cell. Cells and supernatants were collected at the indicated time points for determination of virus titer. Error bars indicate means ± the standard deviation (SD) from three experiments.

doi:10.1371/journal.pone.0058414.g001

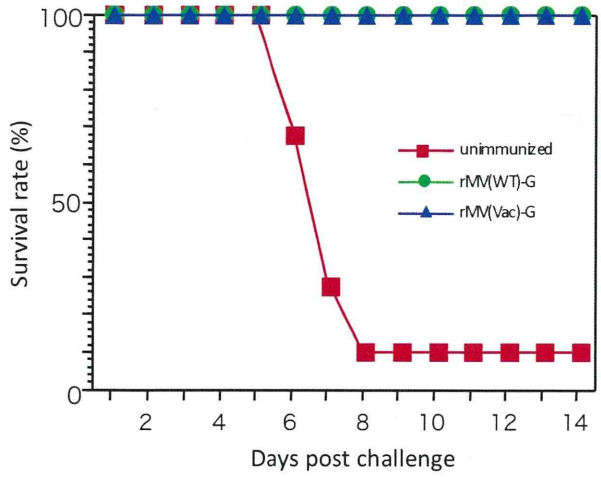

Figure 2. Survival curves of hamsters inoculated with NiV. Hamsters (n = 10) were immunized intraperitoneally with 2×10^4 $TCID_{50}$ of rMV-HL-G or rMV-Ed-G, and boosted with the same dose 3 weeks after the first immunization. Unimmunized hamsters were inoculated with phosphate-buffered saline (PBS). Four weeks after the first immunization, hamsters were challenged intraperitoneally with 2×10^3 $TCID_{50}$ NiV. The survival of each group was observed for 14 days after challenge.
doi:10.1371/journal.pone.0058414.g002

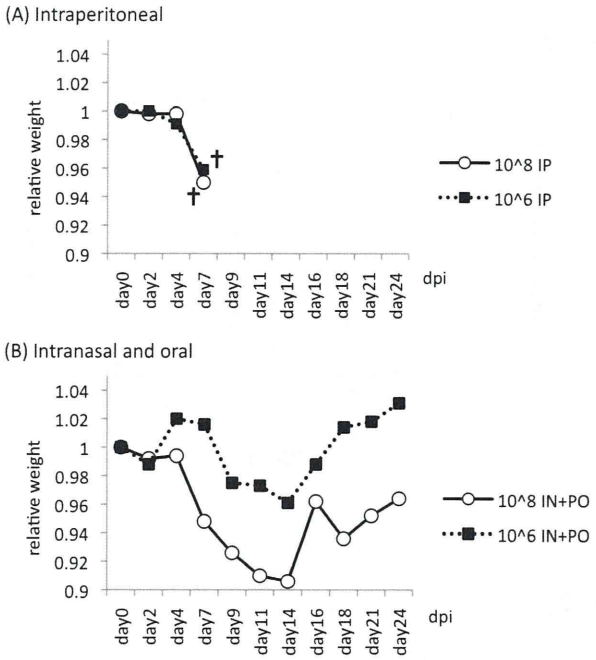

Figure 3. Body weights of Nipah virus-infected monkeys. Each monkey was inoculated with 10^8 or 10^6 $TCID_{50}$ of NiV *via* intraperitoneal (A) or intranasal and oral routes (B). Monkeys were examined every 2–3 days, and body weights recorded. Levels were standardized, with the weight at the first day of the experiment set as 1.
doi:10.1371/journal.pone.0058414.g003

for human use. Efficacy studies in a non-human primate model are required for the development and approval of a new vaccine or antiviral for use in humans. Recently, African green monkey have been shown to be a highly pathogenic model for NiV infection [27]. Pathogenicity of NiV in these monkeys was demonstrated through intratracheal and oral inoculation. When we started to test susceptibility of African green monkeys to NiV, there was no report available. We compared infections resulting from inoculation *via* intraperitoneal or intranasal/oral routes. Our findings show that intraperitoneal inoculation induces a more severe manifestation than intranasal and oral inoculation. However, the intranasal/oral route, which mimics the more natural infection route for humans, did cause severe illness in two infected monkeys by 9–14 dpi. Symptoms were consistent with human NiV infection, and the monkeys became moribund, although they eventually recovered. The progression of illness clinically is similar to human cases. Histopathological tests suggested that when administered *via* an intraperitoneal route, lymphoid organs including spleen and lung were the main target organs of virus propagation. The cause of death was severe respiratory distress resulting from hemorrhage and edema in the lungs, and monkeys died at 7 dpi, which is well before the viral infection could have advanced to the cerebral region of the brain. Although intranasal/oral inoculation also made monkeys ill, we found no evidence of virus propagation or pathological changes, possibly because the samples were taken at the end of the experiment (24 dpi) after the monkeys had recovered. Intranasal/oral inoculation is more natural route for human infection, and induced symptoms in monkeys similar to those observed in humans. However, we decided to use intraperitoneal route for the NiV challenge after immunization with our recombinant MV vaccine because it caused more severe illness and resulted in an earlier death.

A canarypox virus-based vaccine vector has been shown to be effective as a vaccine against NiV-associated disease in veterinary vaccine [15]. The canarypox virus does not replicate in mammalian cells, although it can infect and produce viral proteins. Thus, it is able to eliminate the safety concerns that exist for vaccinia virus vectors. For human use, approaches employing soluble subunit vaccines, virus-like particles, vaccinia virus vectors or complementing defective vesicular stomatitis virus vectors have been explored previously [14,28,29,30,31]. Although they seem promising as vaccines, their efficacy might be problematic because these replication-defective vectors cannot induce long-term immunity.

Live-attenuated measles vaccines have been used since the 1960 s worldwide because they are highly effective and safe. Because MV is an RNA virus, with no DNA intermediates during replication, MV genome does not integrate into host genome. These characteristics make live-attenuated MV vaccines an attractive candidate vector to provide safe and effective immunity against various pathogens. In particular, it induces strong cellular immunity and the effects are long term. For these reasons, many recombinant MVs expressing antigenic proteins of other infectious diseases are under development. It could be argued that the widespread vaccination for measles could result in inactivation of the recombinant MV vector before there is a chance that the NiV G protein can be expressed and induce protective immunity. We examined the antibody responses induced by rMV-Ed-G and rMV-HL-G in MV-seropositive monkeys. Both recombinant MVs could induce specific antibodies; in particular, two inoculation with rMV-Ed-G induced a high titer of a antibodies (1:12800; data not shown). Therefore, it appears that our rMV vaccines are available for people that have been exposed to MV vaccines previously.

In this study, we have demonstrated that recombinant live-attenuated MVs are effective at preventing the onset of symptoms typical of NiV infection. Immunization with recombinant MVs expressing NiV glycoproteins perfectly protected hamsters against